ON EFFECTIVE INPUT MOTIONS:

OBSERVATIONS AND SIMULATION ANALYSES

Michio IGUCHI
Science University of Tokyo, Yamazaki, Noda City 278-8510, JAPAN, iguchi@rs.noda.sut.ac.jp

Yuzuru YASUI
Obayashi Corporation, Shimokiyoto, Kiyose City 204-8558, y.yasui@tri.obayashi.co,jp

and

Chikariro MINOWA
NIED, Tennoudai, Tsukuba City 305-006, minowa@bosai.go.jp

ABSTRACT

The response of a foundation during earthquakes, which includes the effects of inertial and kinematic interactions, is referred to as an effective input motion. It expresses the total interaction effects during earthquakes and will be one of the key factors in the soil-structure interaction study. This paper discusses characteristics of the effective input motion extracted from earthquake observations of 19 events recorded on a large-scale shaking-table-foundation and the surrounding soil. The main findings obtained in this study can be summarized as follows. (1) The characteristics and magnitudes of the horizontal effective input acceleration motions compared to the surface ground motions depend greatly on the frequency components included in the ground motions. (2) The ratios of the vertical effective input motions to the vertical ground motions on the surface show slightly larger than those for the horizontal components. (3) The vertical peak motions at the ends of the foundation due to the rocking motion become as large as a quarter of the vertical peak motion on the soil surface. (4) The characteristics of the effective input motions obtained by the analysis of small to mid ground motions differ in magnitude from those obtained for strong ground motion records of the Hyogo-ken Nambu earthquake, but show the similar in tendency. (5) The effective input motions numerically evaluated on a basis of the free-field motions has shown a good agreement with the observation.

Key Words: SSI, Earthquake observation, Embedded Foundation, Simulation Analysis, Effective Input Motion

1. INTRODUCTION

In assessing the soil-structure interaction (SSI) effects, it would be preferable to express the effects with a simple index. The effects of the inertial interaction may be characterized by changes of the system period and the damping factor compared to those for the base-fixed condition. The kinematic interaction effects, on the other hand, may be characterized by the ratio of the foundation input motions to the free-field motions. But there has been presented no proper index to assess the total interaction effect. It is desired to introduce an appropriate

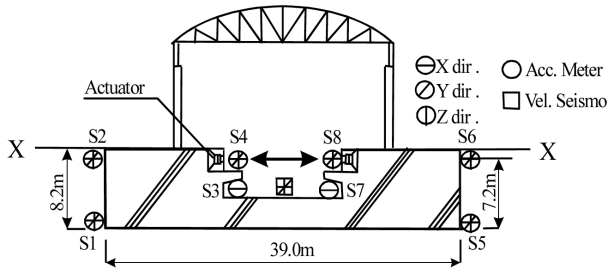

Fig. 1. Outline of Shaking Table Foundation and Location of Seismometers

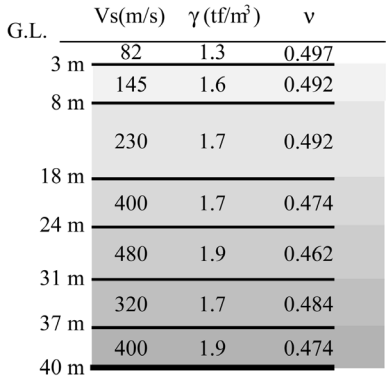

Fig. 2. Soil Profile

index to express the total effects of the SSI, which is measurable directly from observations. The response of a foundation during earthquakes, which may be considered to be an input motion for the superstructure, will be referred to here as the effective input motion (EIM). The EIM includes the effects of both the inertial and kinematic interactions, and consequently can be a synthetic index of the soil-structure interaction effects. The importance of the EIM has been brought into relief by the analyses of intensive seismic motions recorded simultaneously on structures and at the surrounding soil during the 1995 Hyogo-ken Nambu Earthquake [Yasui et al. (1998)]. The evaluation of EIM based on earthquake observations is important not only in clarifying the input mechanism of seismic motions into superstructures but also in assessing the SSI effects on the response of superstructures.

Some characteristics of the EIM have been studied on the basis of analytical procedures and also numerical evaluations [Thau et al. (1974); Iguchi (1984)]. Many attempts to extract the SSI effects from the observed seismic records have been also made extensively [e.g. Ishii et al. (1984); Celebi (1997); Stewart and Fenves (1998)]. In these studies, however, because of insufficient records observed on the structures, the sufficient SSI effects such as rotational components of the input motions have not been extracted from observations. In order to extract the SSI effects from observations, it is required to observe the seismic motions on densely instrumented structures or foundations as well as at the surrounding soil. It is also desirable to observe the seismic motions for various earthquakes for a long time under the same conditions. The observation on such idealized conditions has been scarcely made. The dense observations of seismic motions have been made on several points on a large-scale shaking table foundation in Tsukuba and in the surrounding soil. The objective of this study is to make clear the relationships between the frequency characteristics of ground motions and EIM using 19 sets of the seismic records observed for about six years on the foundation and in the soil

2. OUTLINE OF FOUNDATION AND EARTHQUAKE OBSERVATION

The outline of the foundation is shown in figures 1. The weight of the foundation itself and the shaking table is about 11,600 tf and 180 tf, respectively. The weight of the superstructure is about 200tf. The total weight corresponds almost to the excavated soil of the foundation. The fundamental frequency of the soil-foundation system is about 4.1 Hz in EW direction. It has been confirmed that the foundation behaves as a rigid body within frequencies less than 10 Hz. The fundamental frequency of the superstructure is 3.5Hz. The soil profile at this site is shown in figure 2 together with soil constants of shear wave velocities, densities and Poisson's ratios. These constants were explored by the down-hole PS logging tests. The more detail about the foundation and the soil can be found elsewhere [Minowa et al. (1991); Iguchi et al. (2000)].

Table 1. Parameters of Earthquakes

Eq.No.	Date	Time	Hypocenter (N:N.L., E:E.L.)	Depth (km)	Mag. (M)	Max. of Acc. (gal) (NS)	(EW)	(UD)	Group
2	8.6	23.49	N35.87, E141.15	26	5.8	16.32	10.79	3.85	A
3	10.19	8:31	N36.08, E139.92	59	4.3	43.73	35.76	36.84	C
4	11.19	17:19	N35.60, E140.02	81	4.9	14.78	12.60	4.32	C
5	12.12	11:22	N36.46, E140.66	48	4.6	14.11	16.21	8.34	B
6	1992.2.2	4:04	N35.23, E139.79	92	5.9	23.16	24.84	8.94	B
9	5.11	19:04	N36.53, E140.54	56	5.6	25.71	29.28	23.28	B
10	6.1	22:51	N36.67, E141.27	44	5.7	18.22	20.48	7.82	B
11	8.30	4:19	N33.20, E138.34	325	6.6	18.21	16.30	6.35	B
14	1993.6.7	16:47	N36.02, E141.76	28	5.9	7.02	9.32	2.26	B
16	9.18	11:18	N36.18, E140.88	35	5.0	18.24	16.21	8.95	B
17	10.12	0:55	N32.02, E138.24	390	7.0	27.15	24.96	10.40	B
21	1995.1.7	7:39	N40.18, E142.32	30	6.9	9.82	7.35	3.61	A
22	1.7	21:34	N36.17, E139.59	70	5.4	92.56	100.47	40.83	B
23	1.8	4:38	N36.19, E139.58	72	4.6	12.91	17.01	9.29	C
24	1.10	3:00	N35.56, E141.26	45	6.2	11.08	9.90	4.09	A
27	4.12	14:20	N36.27, E140.37	52	4.6	14.41	13.23	10.69	B
28	7.3	8:53	N35.06, E139.30	120	5.6	6.04	5.80	6.08	B
29	7.30	3:11	N35.54, E140.36	50	5.0	28.47	20.90	16.37	B
30	1996.9.11	11:37	N35.07, E141.03	30	6.6	26.65	26.52	12.15	A

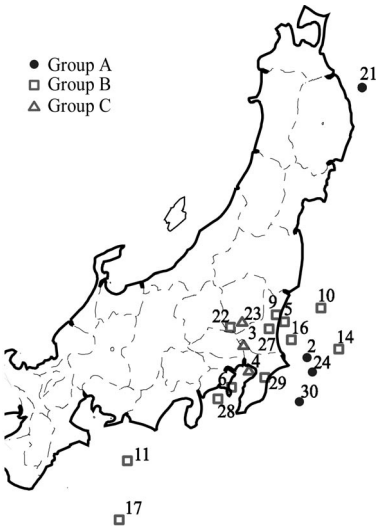

Fig. 3. Location of Hypocenter

The observations of free-field ground motions have been made by three-component accelerometers at the depths of 1m and 40m. The locations are about 100m away from the foundation. We refer to the free-field motions observed at -1m as the surface motions. As for the foundation, the earthquake motions on the foundation have been observed at several points with accelerometers and a velocity seismometer as shown in figure 1. The responses of the foundation are represented by accelerograms recorded at point S4, which is located almost at the center of the foundation and at the same level as the free-field surface motions. The records of about 30 earthquakes had been observed for six years from 1991 to 1996. They included incomplete records and they were omitted from the analyses. The locations of epicenter of 19 earthquakes that were used in the analyses are plotted in figure 3 and the earthquake parameters are shown in table 1. The observed peak accelerations on the free surface in the NS, EW and UD directions have been less than about 30 gals except the event of No. 22 as shown in table 1. Thus, it might be considered that the soil had been within an elastic range during the earthquakes except for the event of No. 22.

3. GROUPING OF OBSERVED SEISMIC RECORDS

In order to analyze the characteristics of the EIM in relation to frequency component, each earthquake was categorized into three groups (groups A, B and C). The grouping was made according to the frequency components included in the earthquake acceleration motions (NS component) on the soil surface; the earthquakes having motions that contain predominantly the lower frequencies less than 1Hz were categorized into group A; the earthquake motions including higher components (more than about 3 to 4Hz) were grouped into C, and group B is characterized by the motions having intermediate frequency components between groups A and C. Thus categorized group for each earthquake is shown in table 1. Figure 4 shows the normalized Fourier spectra

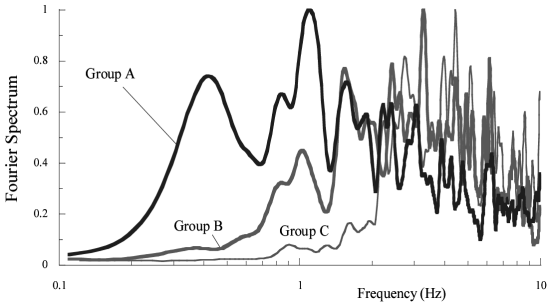

Fig. 4. Normalized Fourier Spectra of Representative Earthquakes.

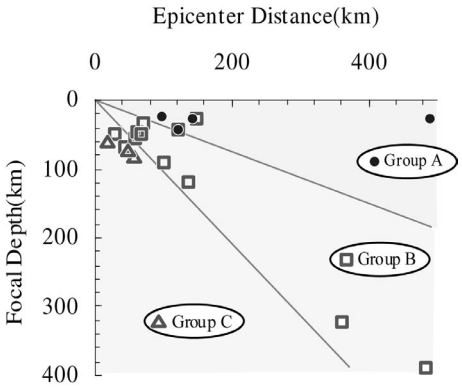

Fig. 5. Epicenter and Focal Depth.

of the representative motions chosen from the respective groups. The spectra were smoothed by using the Parzen's window with a bandwidth of 0.1Hz.

It is interesting to reveal that what earthquake parameters have to do with each group. In figure 5, the hypocenter of each earthquake is plotted in the diagram of epicenter distance to focal depth relation. It may be clearly detected from the figure that the hypocenters of group A are located within a region of the depth to distance ratio being less than 0.4. The hypocenters of the earthquakes of group C, on the other hand, are located about right under the observation point in Tsukuba, and the earthquakes of group B are plotted between the two. These results are suggesting that the frequency component included in the surface motions is strongly related to the ratio of focal depth to epicenter distance.

4. RELATION BETWEEN SURFACE MOTIONS AND EFFECTIVE INPUT MOTIONS

4.1 Relationship between peak accelerations

In the first step of analyses of the observed records, the relationship between the peak values of the surface ground motions and peak responses of foundation (EIM) was studied. Before the analysis, the bearing modification is made for the free-field motions, as the compass directions of the free-field motions are different from the longitudinal and transverse directions of the foundation by 58 degrees.

The relationships between the peak accelerations on the foundation and those on the free surface are plotted for longitudinal (X direction), transverse (Y direction) and vertical directions in figures 6(a), (b) and (c), respectively. The lines in the figures are the slopes drawn for the respective groups based on the least-squares method. The slopes may be interpreted as the average ratios of the peaks of the EIM to the free surface motions. We refer to the slopes as effective input coefficients (EIC) of acceleration. The EIC of acceleration are shown in table 2 together with the correlation coefficient (C.C.). These results are indicating that the EIC decrease in the order of groups A, B and C in the X direction. In other words, the input loss tend to be remarkable, as the higher

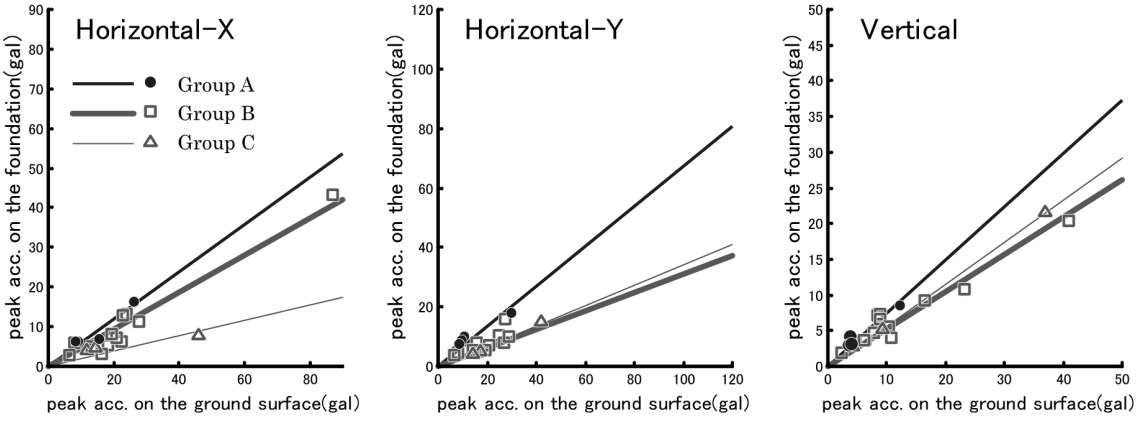

(a) X-direction (b) Y-direction (c) Vertical

Fig. 6. Relationship between Peak Accelerations of Surface Ground Motions and Foundation.

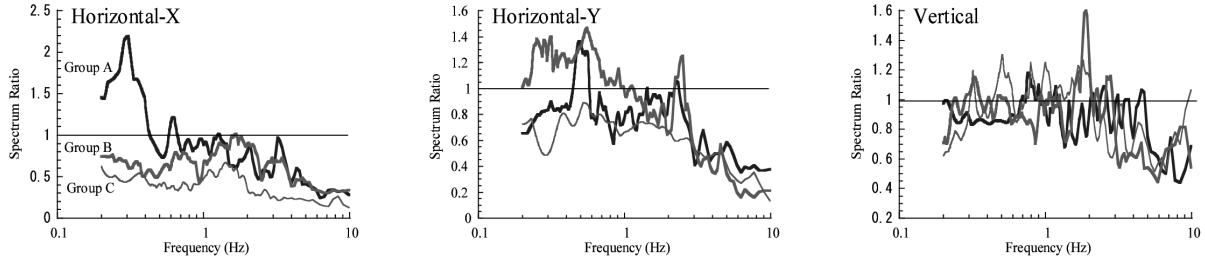

(a) X-direction (b) Y-direction (c) Vertical

Fig. 7. Response Ratios of Acc. Motions on Soil Surface to Those on Foundation

frequencies contained in the free surface motions become more pronounced. On the other hand, the EIC in the Y direction are larger than those of the X direction for group A. It is also noticed that the EIC of groups B and C are showing the same slopes in contrast to the case of the X direction. The different tendency in the X and Y directions is attributed to the motions of No.22 earthquake that have influenced greatly on the slope of group B and in the Y direction. If we exclude the point of the earthquake from the analyses, the tendencies in the Y direction are almost the same as in the X direction. The vertical EIC are shown in figure 6(c) and table 2. The difference among the groups is less pronounced than the case of the horizontal results. The EIC of the vertical components increase in the order of groups A, C and B, whose order is different from the case of horizontal motions. It should be noted that the EIC obtained in this study are remarkably small compared with the results obtained for the 1995 Hyogo-ken Nambu Earthquake, in which the slope of acceleration was 0.7 [Yasui et al. 1998]. The main reason of the different slopes is due to the difference of the frequency components included in the motions observed at this site from those during the Hyogo-ken Nambu Earthquake. Another reason is related to the amplification of acceleration near the surface layers of about 8m thick, which will be discussed afterward.

4.2 Response spectrum ratio

Figures 7(a), (b) and (c) show the ratios of response spectra for acceleration motions of the foundation to those of the free surface. These are the results for the representative motions chosen from the respective groups and for the X, Y and vertical directions. The damping factor was 5%. The followings will be noticed. (1) The spectrum ratios for the horizontal components tend to decrease with increase of frequencies up to 10Hz. The ratios exceed 1 in lower frequencies in the X and Y directions of group A and also in the Y direction of group B. (2) As for the vertical component, the ratios tend to be more than 1 in wider frequency range irrespective of the groups.

It might be worth noticing that the spectrum ratios of the horizontal components are different among the groups as seen, e.g. in the X direction of the groups A and B. It will be infered that if input-output relationship between

Table 2. Effective Input Coefficients of Acceleration

Group	Horizontal-X		Horizontal-Y		Vertical	
	Cof. of EIM	C.C.	Cof. of EIM	C.C.	Cof. of EIM	C.C..
Group A	0.60	0.93	0.67	0.99	0.74	0.98
Group B	0.47	0.97	0.31	0.97	0.52	0.97
Group C	0.20	0.99	0.34	1.00	0.59	1.00
Whole Av.	0.43	0.90	0.33	0.92	0.55	0.97

Table 3. Effective Input Coefficients of Velocity

Group	Horizontal-X		Horizontal-Y		Vertical	
	Cof. of EIM	C.C.	Cof. of EIM	C.C.	Cof. of EIM	C.C.
Group A	0.72	1.00	0.95	0.97	0.90	0.98
Group B	0.76	1.00	0.55	0.95	0.69	0.90
Group C	0.29	0.32	0.43	1.00	1.02	0.95
Whole Av.	0.73	0.99	0.72	0.89	0.79	0.93

the free-field motions at every point around the foundation and the response of the foundation is constant despite the difference of the incoming waves, then the ratio must be the same for different groups. But the results of groups A and B are showing differently as seen from figures 7(a) and (b). This might be indicating that the relation between the free field motions and the foundation response is a multi-input system. The different response ratios between groups A and B, e.g. in the frequencies around 0.2 to 0.7 Hz, might be understood to have been attributed to the different distribution of the seismic ground motions around the foundation. The spectrum ratios shown in figures 7(c), on the other hand, are almost the same for different groups. This might be suggesting that the vertical distribution of the free field motions around the foundation is almost same for different groups.

4.3 Relation between the peak velocities

The same examinations were made for the peak velocities between the free surface motions and the foundation. The velocity motions were obtained by numerical integrations. The relationship between the peak velocities of the surface motion and the foundation are shown in figures 8(a), (b) and (c), respectively. In these figures, the straight lines are drawn for the respective groups and the slopes are summarized in table 3. These results are indicating that the EIM of velocity were around 0.7 and 0.8 in the X direction for groups A and B. These values are larger than those for accelerations. It may be noticed from the table 3 that the slopes decrease in the order of groups A, B and C in the Y direction, which are larger than those for the X direction. These tendencies are coincide with the results obtained from the observations during the 1995 Hyogo-ken Nambu Earthquake [Yasui et al. 1998].

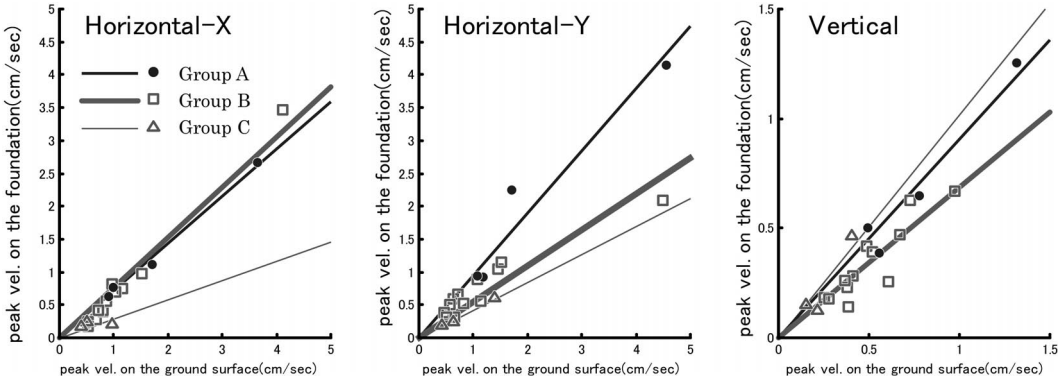

(a) X-direction (b) Y-direction (c) Vertical

Fig. 8. Relationship between Peak Velocities of Surface Ground Motions and Responses of Foundation

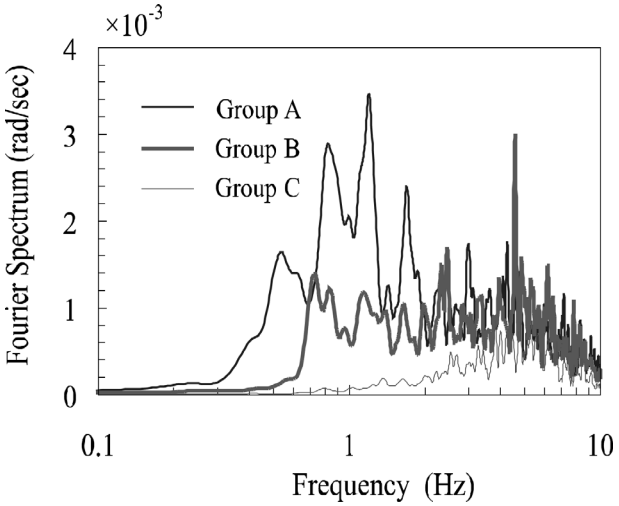

Fig. 9. Fourier Spectra of Roking Motions of Foundation

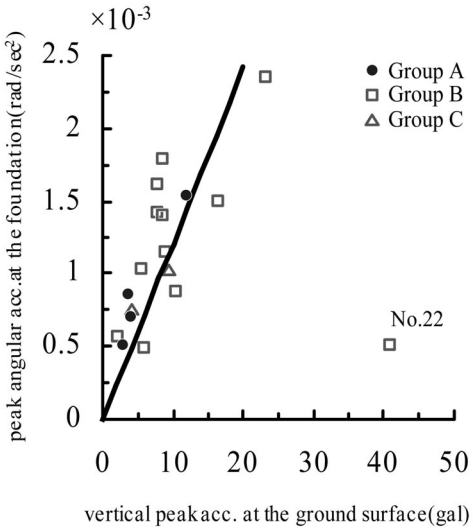

Fig. 10. Peak Acc. of Surface Ground Motion and Peak Angular Acc.

4.4 Effective input motions of rotational component

The rocking acceleration motions with respect to the Y-axis were extracted from the vertical observations at the both ends of the foundation (S1, S2, S5 and S6 shown in figure 1). Figure 9 shows the Fourier spectra of the rocking accelerations corresponding to the representative motions chosen from the respective groups. The results shown in figure 9 are characterized by higher frequency components included in the rocking motions, comparing to the results for the horizontal components shown in figure 4.

Figure 10 shows the relationship between the vertical peak accelerations on the soil surface and the peak values of the rocking motions of the foundation. As seen from figure 10, the rocking motions are strongly correlated to the vertical ground motions. The slope of the straight line obtained excluding the event No. 22 was b=0.12x10^{-3}rad/sec^2/gal. This indicates that the vertical motions at the ends of the foundation associated with the rocking motion are about 1/4 of the vertical motions in average on the soil surface.

Finally, we will refer to an interpretation of the result that the rocking motion for the event No. 22 was small compared to the vertical motion. It may be considered that horizontal forces applied on the sides of the foundation would mainly induce the rocking motions of the foundation. The deterioration of rigidity in the lateral soil of the foundation, because of high strain level in the soil for No.22 event, could have decreased the forces applied on the lateral sides during the earthquake.

5. FREE-FIELD MOTIONS AND EFFECTIVE INPUT MOTIONS

5.1 Estimation of free-field motions

In order to make clear the input mechanism of ground motions into the foundation, the free-field motions in the soil were numerically estimated on a basis of the observed motions on the soil surface and at depth of 40m. In the numerical analysis, the soil was assumed to be horizontal layering soil, and the vertical incidence of S-wave from the bottom of the soil model was also assumed. The Thomson-Haskell method was employed in the analysis. As for the soil constants such as shear wave velocity, density and Poisson's ratio of each layer, the explored results shown in figure 2 were used without giving any modification to them. The damping constants of the soil were assumed to be hysteretic type and the values were determined by trial and error, so that the

calculated motions at the depth of 40m coincided with the observed motions. Thus determined complex shear modulus was as follows [Ohsaki (1994)].

$G^* = G\,(1 + 2\,i\,h)$ (1)

where

$h = \alpha / \omega + \beta$ (2)

with $\alpha = 1.0\ \mathrm{sec}^{-1}$ and $\beta = 0.02$.

In figures 11(a) and (b) the numerically evaluated acceleration motions in the X direction are compared with the observations for the representative earthquake motions of groups A and B. The fairly good agreement between these two was obtained. Though not shown in figure, for the group C in which higher frequencies were predominant, the agreement was not so good as the cases of groups A and B.

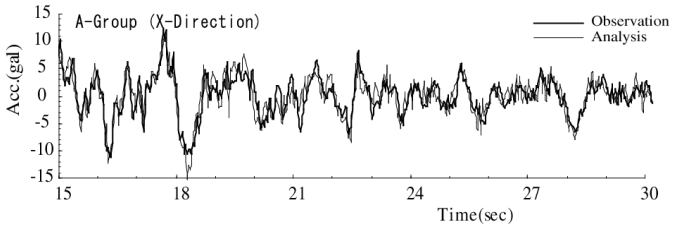

(a) Group A (X-direction)

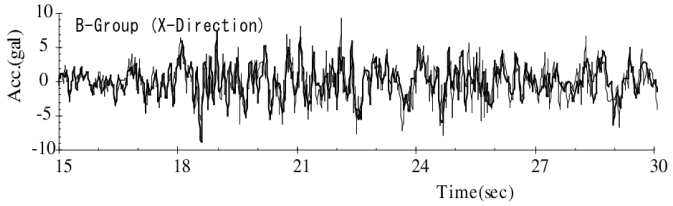

(b) Group B (X-direction)

Fig. 11. Comparison between the Observed and Analysis

The shear strains in each layer were numerically evaluated for motions of the representative earthquakes and of event No. 22 that had shown the maximum acceleration among the recorded motions. The maximum strains are shown in table 4. It might be observed that the peak strains have appeared in the top layer and were about 0.5×10^{-4} to 0.8×10^{-4} except for the event No. 22. The soil might have been within elastic limit during the earthquakes. As for the case of the event No. 22 on the other hand, the peak strains have reached 1.6×10^{-4} to 2.5×10^{-4} and the soil in the top layer might have a possibility to have exceeded the elastic limit [Ishihara (1996)]. The peak amplification factors on the soil surface to the motions at the depth of 8m were 1.5, 2.4 and 2.5 for the groups A, B and C, respectively. The high amplification factors for the groups B and C may be considered to be relating to the fundamental frequency of the top layers. The fundamental frequency of the surface layers was 3.5Hz, that was approximated by $f_1 = (4H_1/V_{s1} +$

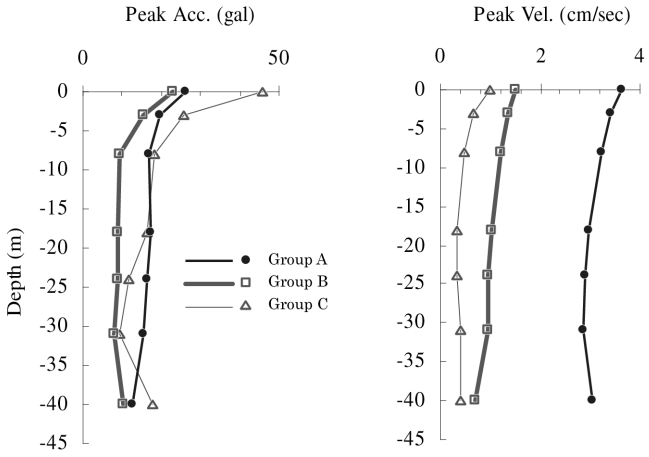

(a) Acceleration. (b) Velocity.

Fig. 12. Distribution of Peak Motions along Depth

Table 4. Maximum Shear Strain at Each Soil Layer (x 10^{-4})

Layer No.	A Group		B Group		C Group		Eq. No. 22	
	X-Dir	Y-Dir	X-Dir	Y-Dir	X-Dir	Y-Dir	X-Dir	Y-Dir
1	0.57	0.57	0.45	0.58	0.78	0.71	1.61	2.54
2	0.50	0.52	0.36	0.37	0.33	0.48	1.05	1.71
3	0.41	0.42	0.22	0.25	0.20	0.19	0.77	0.82
4	0.20	0.21	0.10	0.12	0.06	0.08	0.36	0.30
5	0.15	0.16	0.07	0.08	0.04	0.06	0.28	0.21
6	0.45	0.50	0.21	0.22	0.10	0.17	0.76	0.54

$4H_2/V_{s2})^{-1}$ with H_1 and H_2 being the thickness of top two layers.

5.2 Amplification of ground motions in the top layers

It was inferred in the preceding section that the small values of the EIC of acceleration shown in table 2 might be attributed to the amplification of the ground motions in the top layers. In order to prove the inference, the peak accelerations and velocities along the depth of soil were numerically evaluated with use of the soil parameters shown in figure 2. The results are shown in figures 12(a) and (b). As seen from these results, the accelerations are amplified remarkably near the surface layers especially for the groups B and C. This fact might have lead to small values of EIC of acceleration shown in table 2.

From distribution of the velocity motions along depth of soil shown in figure 12(b), it will be noticed that the amplifications in the surface layers are less pronounced than the accelerations. The amplification factors on the soil surface to the motions at the depth of 8m were 1.1, 1.2 and 1.9 for the groups A, B and C, respectively.

5.3 Free-field motions at the level of foundation base and effective input motions

As being easily presumed, the motions affecting mostly on the EIM would be the free-field motions at the level of the foundation base since a foundation is usually supported on a firm soil. The fact that the motions at the level of foundation base are almost same as the response of foundation had been known through numerical studies of the soil-structure system [Seed and Lysmer (1978)]. This was also inferred by analyses of the observed motions recorded during Hyogo-ken Nambu Earthquake [Yasui et al. (1998)]. In order to examine the hypothesis, the relation between the peak accelerations observed on the foundation and those of free-field motions at the depth of 8m were studied. The compared results of the peak accelerations are shown in figures 13(a) and (b). In figure 14(a) and (b), the relationship about the peak velocities are plotted. The lines were drawn by the linear regression analysis. The slopes of these lines (EIC) are summarized in table 5 together with the correlation coefficients (C.C.) for each group and direction. It is apparently noticed that the difference of the results shown in tables 2 and 5 is remarkable. The difference of the EIC between two results might have been caused by the constraint effect of the rigid embedded foundation to the motions along the sides of the foundation. This effect may be interpreted as the kinematic interaction.

It may be noticed from figure 13 that while the slope of the EIC of acceleration for group C was 0.48, the slopes for groups A and B were 0.85 to 1.06 in the X direction, whose values are larger than the corresponding results shown in table 2. These results are suggesting that the input of seismic motions into the foundation was predominant from the base of the foundation and less from the lateral sides of the foundation for X direction. In

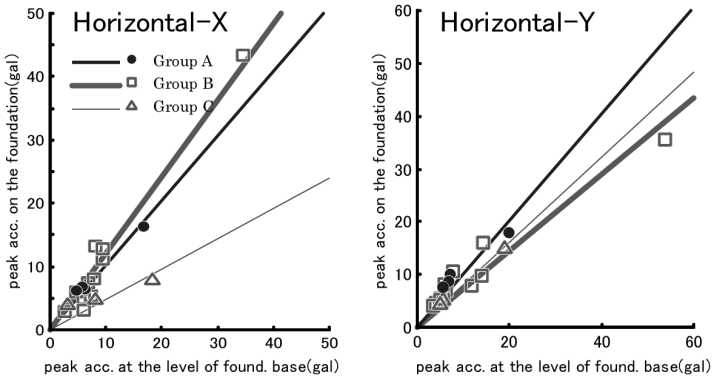

(a) X-direction (b) Y-direction

Fig. 13. Peak Accelerations of Free Field Motions at the Level of Foundation Base and Peak Response of Foundation

Table 5. Effective Input Coefficients of Acceleration and Velocity

Group	Acceleration				Velocity			
	Horizontal-X		Horizontal-Y		Horizontal-X		Horizontal-Y	
	Cof. of EIM	C.C.	Cof. of EIM	C.C.	Cof. of EIM	C.C.	Cof. of EIM	C.C.
Group A	1.02	0.99	1.01	0.99	0.81	0.99	0.99	0.98
Group B	1.21	0.98	0.72	0.97	1.10	0.99	0.98	0.97
Group C	0.48	0.99	0.80	1.00	0.56	0.24	1.23	0.95
Whole Av.	1.06	0.91	0.76	0.97	0.94	0.95	0.99	0.98

the Y direction on the other hand, the EIC for the group B showed smaller value comparing to that of X direction. In the same manner, observing the results shown in figures 14(a) and (b) the EIC of velocity are about the same or larger than those of acceleration shown in figures 13(a) and (b). The slopes shown in figures 14(a) and (b) are the averaged results of the whole data, and are 0.94 for X direction and 0.99 for Y direction.

6. SIMULATION ANALYSIS OF EFFECTIVE INPUT MOTIONS

6.1 Method of analysis

The simulation analysis of the effective input motions was performed on a basis of an approximate method proposed by Iguchi [Iguchi (1982)], and modified by some others [Takemiya and Wang (1988); Kurimoto and Iguchi (1995)]. Let $\{U^*\}=\{\Delta_x^*, \Phi_y^*\}^T$ be the horizontal and rotational responses at the base of a massless foundation when subjected to the harmonic seismic waves with a circular frequency ω be, then the responses may be approximately expressed as follows [Kurimoto and Iguchi (1995)].

$$\{U^*\} \approx [H]^{-1} \int_S [A(\bar{X})]^T \{u^f(\bar{X})\} dS \quad -\omega^2 [K]^{-1} \int_V \rho(X) [A(X)]^T \{u^f(X)\} dV, \quad \bar{X} \in S, \quad X \in V \tag{3}$$

where S is the area of the interface between a rigid foundation and soil, V is the volume of soil occupied by the foundation, $\bar{X}(x_s, y_s, z_s)$ is the coordinate on the surface S, $\{u^f\}$ is the free-field motions, $\rho(X)$ is the mass density of soil, and $[A(\bar{X})]$ is a coordinate transformation matrix which is expressed as follows.

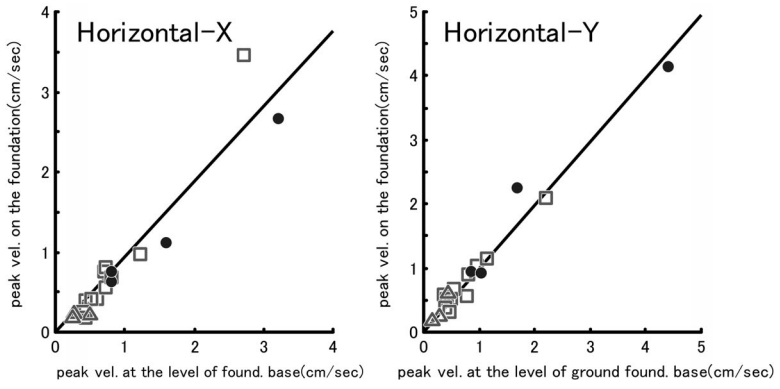

(a) X-direction (b) Y-direction

Fig. 14. Peak Velocities of Free Field Motions at Level of Foundation and Peak Response of Foundation

$$[A(\bar{X})]=\begin{bmatrix}1 & z_s\\ \cdot & -x_s\end{bmatrix} \tag{4}$$

Furthermore, $[H]$ and $[K]$ are the shape matrix and the impedance matrix of the foundation, respectively, as defined below.

$$[H]=\int_S [A(\bar{X})]^T [A(\bar{X})]dS \tag{5}$$

$$[K]=\begin{bmatrix}K_{HH} & K_{HM}\\ K_{MH} & K_{MM}\end{bmatrix} \tag{6}$$

The impedance matrix for this shaking table foundation had been obtained by the thin layered method as shown in figure 15 [Kobayashi (1993)]. The results are defined at the center of the base. The response at the base center of the foundation including the effect of the mass may be calculated by

$$\begin{Bmatrix}\Delta_x\\ \Phi_y\end{Bmatrix}=\left([E]-\omega^2\begin{bmatrix}K_{HH} & K_{HM}\\ K_{MH} & K_{MM}\end{bmatrix}^{-1}\begin{bmatrix}M & Mh_G\\ Mh_G & J_0+Mh_G{}^2\end{bmatrix}\right)^{-1}\begin{Bmatrix}\Delta_x^*\\ \Phi_y^*\end{Bmatrix} \tag{7}$$

where M, J_0 are the mass and mass moment of inertia with respect to the axis through the axis of the foundation, h_G is the height of the centroid of the foundation from the base, and $[E]$ is the unit matrix.

6.2 Comparison of analyses and observations

The EIM for the representative earthquakes chosen from the respective groups were numerically evaluated on a basis of the procedure described above. In the calculation, the frequencies more than 10Hz were neglected because of the limited frequency range available for the impedance functions. The computed time histories of the EIM in the X direction compared with the observations are shown in figures 16(a) and (b). Fairly good agreement between the calculated and observed results was obtained for the Groups A and B though limited to small to mid earthquakes. Though not showing in the figure, the agreement between the two for the motion of Group C was not good as those shown in figures 16(a) and (b). This is simply because of having cut the frequencies more than 10 Hz. In figures 17(a), (b) and (c) the Fourier spectra of the computed EIM are compared with those of the observed motions in the X direction of the respective groups.

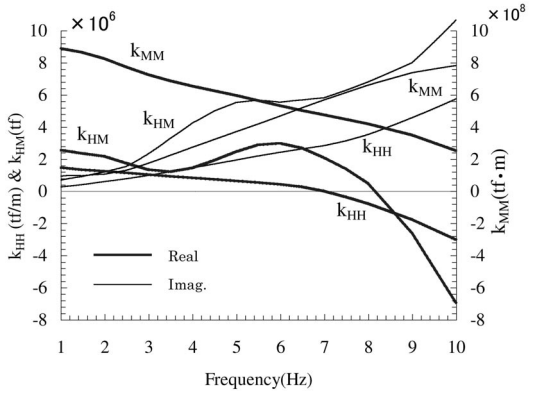

Fig. 15. Impedance Functions

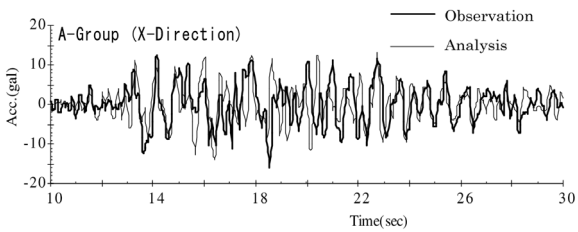

(a) Group A

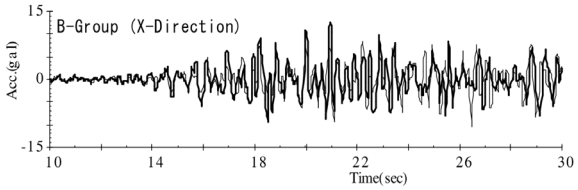

(b) Group B

Fig. 16. Comparison of Effective Input Motion between the Observed and Analysis

7. CONCLUDING REMARKS

The 19 sets of seismic records observed on a large shaking table foundation and at the surrounding soil were analyzed from the standpoint of SSI effects. As an index to assess the SSI effects, the effective input motions were introduced and the characteristics of the index were discussed. The main findings obtained in this study can be summarized as follows.

(1) The characteristics and magnitude of the horizontal effective input motions compared to the surface ground motions have shown to be depending greatly on the frequency components included in the free-field motions.

(2) The ratios of the vertical effective input motions to the vertical ground motions on the surface were slightly larger than those for the horizontal components.

(3) The vertical peak motions at the ends of the foundation due to the rocking motion were as large as a quarter of the vertical peak motion on the soil surface.

(4) The characteristics of the effective input motions obtained by the analysis of small to mid ground motions differed in magnitude from those obtained for strong ground motion records of the Hyogo-ken Nambu earthquake, but have shown the similar in tendency.

(5) The comparison of the effective input motions numerically evaluated on a basis of the free-field motions has shown a good agreement with the observations.

Acknowledgement

The authors wish to express their gratitude to Mr. T. Mutoh of Science Univ. of Tokyo for his helpful corporation in drawing the figures.

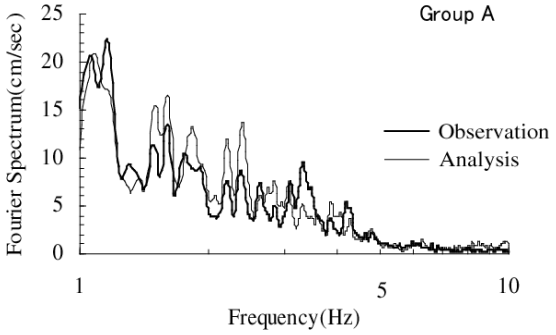

(a) Group A

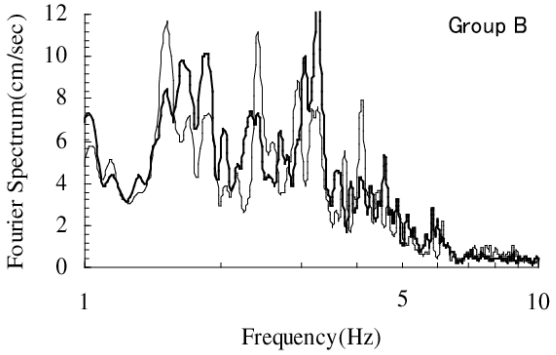

(b) Group B

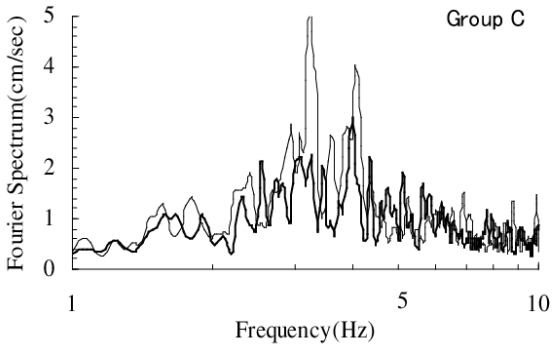

(c) Group C

Fig. 17. Comparison of Fourier Spectrum of Effective Input Motion between the Observed and Analysis

REFERENCES

Architectural Institute of Japan (1996): *An introduction to dynamic soil-structure interaction* (in Japanese), Architectural Institute of Japan.

Celebi, M. (1996): "Response of Olive View Hospital to Northridge and Whittier Earthquakes," J. Struct. Engng, ASCE, Vol. 123, No. 4, pp389-396.

Fukuwa, N., K. Naraoka, K. Watanabe, K. Shiotani and C. Minowa (1988): *Report on dynamic characteristics of large-scale shaking table foundation and the surrounding soil* (in Japanese), Research Report of Ohsaki Research Institute, 88-14.

Iguchi, M. (1982): "An Approximate Analysis of Input Motions for Rigid Embedded Foundations," Trans. Architectural Institute of Japan, No. 315, pp61-75.

Iguchi, M. (1984): "Earthquake Response of Embedded Cylindrical Foundations to SH and SV waves," Proc. 8th World Conf. on Earthq. Engng, Vol. 3, pp1081-1088.

Iguchi, M., H. Kobayashi and C. Minowa (1994): "Experiment versus Theory of Dynamic Characteristics of a Large Shaking Table Foundation and the Surrounding Soil, " Proc. 9th Japan Earthquake Engng Symp., Vol. Ⅲ, ppE283-E288.

Iguchi, M., M. Unami, Y. Yasui and C. Minowa (2000): "A Note on Effective Input Motions Based on Earthquake Observations Recorded on a Large Scale Shaking-Table-Foundation and the Surrounding Soil," J. Struct. Constr. Engng, AIJ, No. 537, pp61-68.

Ishihara, K. (1996): *Soil behaviour in earthquake geotechnics*, Oxford Science Publications, Clarendon Press, p17.

Kurimoto, O. and M. Iguchi (1995): "Evaluation of Foundation Input Motions Based on Observed Seismic Waves," J. Struct. Constr. Engng, AIJ, No. 472, pp67-74.

Kobayashi, H. (1993): *Verification study on dynamic interaction of soil and embedded foundation* (in Japanese), Ms D. Dissertation, Faculty of Science and Engng, Science Univ. of Tokyo (in Japanese).

Minowa, C., Ohyagi, N., Ogawa, N., and Ohtani, K. (1991): *Response data of large shaking table foundation during improvement works* (in Japanese), Technical Note of the National Research Institute for Earth Science and Disaster Prevention, No. 151.

Ohsaki, Y. (1994): *New: Introduction to Spectrum Analysis of Ground Motions* (in Japanese), Kajima Pub. Co., p174.

Seed, H. B. and J. Lysmer (1978): "Soil-Structure Interaction Analyses by Finite Elements –State of the Art- ," Nuclear Engng and Design, Vol. 46, pp349-365.

Takemiya, H. and G. Y. Wang (1988): "A Modified Indirect Boundary Element Method to Compute the Impedance Functions for Rigid Foundations," Proc. 9th World Conf. on Earthq. Engng, Tokyo-Kyoto (Japan), Vol. Ⅲ, pp355-360.

Thau, S. A., A. Umek and R. Rostamian (1774): "Seismic Motion of Buildings with Buried Foundations," J. Engng Mech. Div., ASCE, Vol. 100, No. EM5, pp919-933.

Yasui, Y., M. Iguchi, H. Akagi, Y. Hayashi and M. Nakamura (1998): "Examination on Effective Input Motion to Structures in Heavily Damaged Zone in the 1995 Hyogo-Ken Nanbu Earthquake," J. Struct. Constr. Engng, AIJ, No. 512, pp111-118.